Electronic Supplementary Information

for

Reactivity of Ferrihydrite and Ferritin in relation to surface structure, size, and nanoparticle formation studied for phosphate and arsenate

Tjisse Hiemstra*

*Department of Soil Quality, Wageningen University, P.O. Box 47, 6700 AA Wageningen, The Netherlands. Telephone: + 31 317 48 2342, Fax: + 31 317 41 9000
Correspondence to: tjisse.hiemstra@wur.nl

and

Wei Zhao [# $]

State Key Laboratory of Soil Erosion and Dryland Farming on the Loess Plateau, Northwest A & F University, Yangling, Shaanxi Province 712100, P. R. China

[$] On leave at Wageningen University

CONTENT

1 Electrical double layer structure.

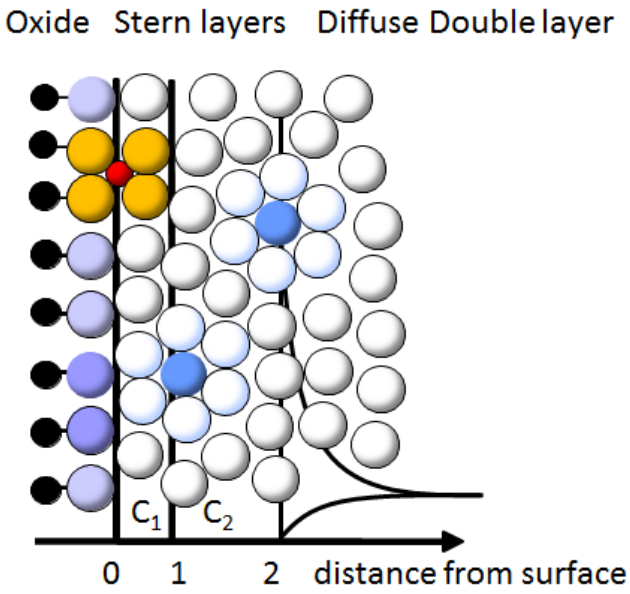

Figure S1. Double layer structure showing a metal (hydr)oxide with surface oxygens (purple) coordinating to metal ions (black) of the solid. The surface oxygens carry an excess proton charge that is compensated by hydrated counter- and co-ions (blue spheres). These electrolyte ions are present in the compact part of the electrostatic double layer or as ions in the diffuse double layer (DDL). The charge of the outer sphere complexes is located at the electrostatic 1-plane that is separated from the surface (0-plane) by the inner Stern layer with a capacitance value C_1, and from the head end of the diffuse double layer by an outer Stern layer with a capacitance C_2. In addition, specifically adsorbing ions (orange/red) may bind as an innersphere complex that has some ligands common with the surface. The charge of these ions is distributed over the 0- and 1-plane. The electrostatic double layer (EDL) structure is known as an extended Stern (ES) layer model.

2 Tableau defining the primary surface reactions of Fh.

Table S1. Ion charge is attributed to the surface (Δz_0) and 1-plane (Δz_1), no charge is added to the 2-plane (Δz_2=0). The Extended Stern layer model has two capacitance values. The values C_1=1.15 F/m^2 and C_2=0.9 F/m^2 are for spherical Stern layers [1]. The overall site densities for ≡FeOH(a), ≡FeOH(b), and ≡Fe_3O are respectively N_{s1}= 3.0 nm^{-2}, N_{s2} = 2.8 nm^{-2}, and N_{s3} = 1.4 nm^{-2}.

Species*	≡FeOH$^{-1/2}$(a)	≡FeOH$^{-1/2\$}$(b)	≡$Fe_3O^{-1/2}$	Δz_0	Δz_1	Δz_2	H^+	Na^+	Cl^-	NO_3^-	ClO_4^-	log$K$*
≡ $FeOH_2^{+1/2}$	1	0	0	+1	0	0	1	0	0	0	0	logK_H = +8.1
≡ FeOH$^{-1/2}$-Na^+	1	0	0	0	+1	0	0	1	0	0	0	logK_{Na} = -0.60
≡ $FeOH_2^{+1/2}$-Cl^-	1	0	0	+1	-1	0	1	0	1	0	0	logK_H+logK_{Cl} = +7.65
≡ $FeOH_2^{+1/2}$-NO_3^-	1	0	0	+1	-1	0	1	0	0	1	0	logK_H+logK_{NO3} = +7.42
≡ $FeOH_2^{+1/2}$-ClO_4^-	1	0	0	+1	-1	0	1	0	0	0	1	logK_H+logK_{ClO4} = +6.7
≡ $FeOH_2^{+1/2}$	0	1	0	+1	0	0	1	0	0	0	0	logK_H = +8.1
≡ FeOH$^{-1/2}$-Na^+	0	1	0	0	+1	0	0	1	0	0	0	logK_{Na} = -0.60
≡ $FeOH_2^{+1/2}$-Cl^-	0	1	0	+1	-1	0	1	0	1	0	0	logK_H+logK_{Cl} = +7.65
≡ $FeOH_2^{+1/2}$-NO_3^-	0	1	0	+1	-1	0	1	0	0	1	0	logK_H+logK_{NO3} = +7.42
≡ $FeOH_2^{+1/2}$-ClO_4^-	0	1	0	+1	-1	0	1	0	0	0	1	logK_H+logK_{ClO4} = +6.7
≡ $Fe_3OH^{+1/2}$	0	0	1	+1	0	0	1	0	0	0	0	logK_H = +8.1
≡ $Fe_3O^{-1/2}$-Na^+	0	0	1	0	+1	0	0	1	0	0	0	logK_{Na} = -0.60
≡ $Fe_3OH^{+1/2}$-Cl^-	0	0	1	+1	-1	0	1	0	1	0	0	logK_H+logK_{Cl} = +7.65
≡ $Fe_3OH^{+1/2}$-NO_3^-	0	0	1	+1	-1	0	1	0	0	1	0	logK_H+logK_{NO3} = +7.42
≡ $Fe_3OH^{+1/2}$-ClO_4^-	0	0	1	+1	-1	0	1	0	0	0	1	logK_H+logK_{ClO4} = +6.7
	ρ_{sus} A N_{s1}[&]	ρ_{sus} A N_{s2}[&]	ρ_{sus} A N_{s3}[&]	Σ_1[&]	Σ_2[&]	Σ_3[&]	H_{tot}	Na_{tot}	Cl_{tot}	NO_{3tot}	ClO_{4tot}	

[§] Doubly-coordinated sites (≡ Fe_2OH^0) are assumed not to contribute to the surface charge.

* Ion pair formation constants are from Hiemstra and van Riemsdijk [2] except the constant for ClO_4 which is from Rietra et al. [3]

[&] Defined in Hiemstra and van Riemsdijk [4].

3 MO/DFT computations. The geometries of the doubly protonated complex of phosphate and arsenate (MH_2) have been optimized with MO/DFT computations. Hydration was explicitly included by initially coordinating two water molecules to each outer ligand of PO_4 or AsO_4 via H bonds. The optimized geometries of both complexes are visualized in Figure S2.

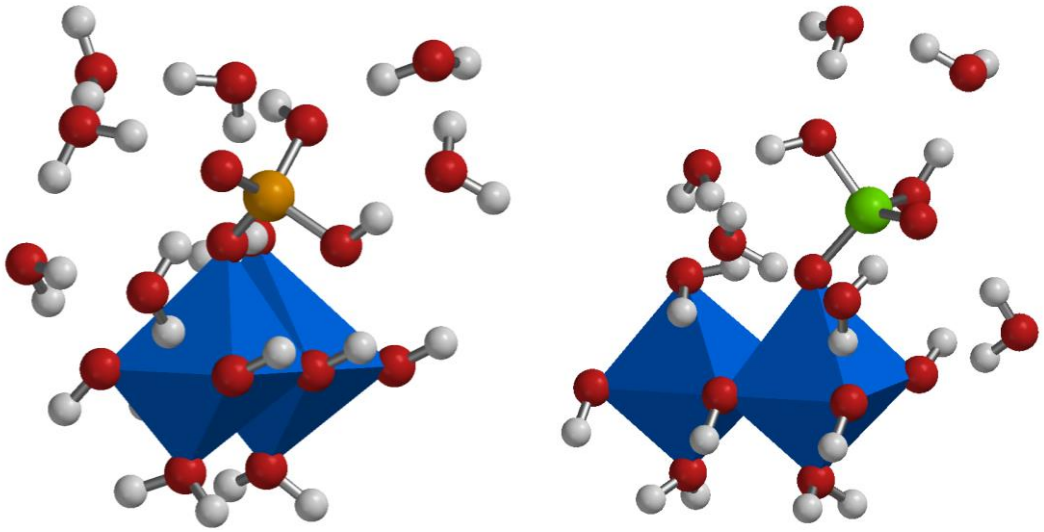

Figure S2. MO/DFT optimized geometry of the structure of a doubly protonated monodentate complex of phosphate (left) and arsenate (right) explicitly hydrated by six additional water molecules interacting with the ligands of the monodentate complex.

In Table S2, the relevant bond lengths (pm) of the ≡FeOPO(OH)$_2$ and ≡FeOAsO(OH)$_2$ complex have been given and the related bond valence ν (v.u.) has been found by applying the Brown bond valence equation:

$$\nu = \exp\left(-\frac{R - \mathrm{R_0}}{\mathrm{B}}\right) \qquad \text{(S1)}$$

in R_o is a reference distance and B a constant (37 pm).

Table S2. Relevant bond lengths in the optimized structures of Figure S2 and corresponding bond valences ν calculated with eq. S1 using the calibrated R_o values given.

Bond	distance (pm)	ν (v.u)	Bond	distance (pm)	ν (v.u)
FeO-P	157.5	1.30	FeO-As	171.7	1.30
P=O	152.5	1.45	As=O	166.2	1.51
P-OH	163.3	1.11	As-OH	178.8	1.06
P-OH	163.5	1.10	As-OH	176.9	1.13
Fe-P	326.7*		Fe-As	339.0	
R_o	167.17		R_o	181.33	

*In agreement with the value reported by Kubicki et al. [5], i.e. Fe-P = 326 pm

The bond valences coefficients n_0 and n_1 have been corrected for interfacial water dipole orientation resulting in the charge distribution coefficients Δz_0 and Δz_1. This is given in Table S3.

Table S3. The charge distribution (n_o and n_1) in MH_2 complexes of phosphate and arsenate with the contribution of the protons involved in the formation reaction starting from $FeOH^{-1/2}$ as reference group. After a small dipole correction [2], the charge distribution coefficients follow (Δz_0 and Δz_1).

	≡FeOPO(OH)$_2$	≡FeOAsO(OH)$_2$
n_0+n_{H0}	-0.70+1 = +0.30	-0.70+1 = +0.30
n_1+n_{H1}	-2.30+2 = -0.30	-2.30+2 = -0.30
Δz_0	+0.33	+0.33
Δz_1	-0.33	-0.33

4 Additional Phosphate adsorption data for Ferrihydrite. The adsorption of phosphate by Fh has also been measured by Tiberg et al. [6] comprising a range of experimental data collected by various contributors. The data have been included successfully in the present parametrization of the CD model (Table 2 of the main text).

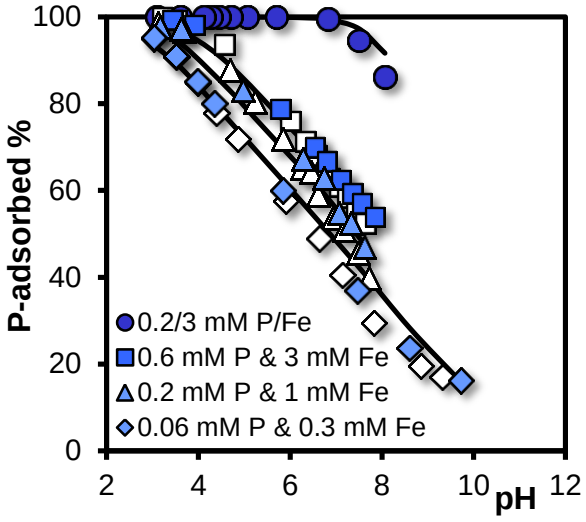

Figure S3. Phosphate adsorption edges in 0.01 M $NaNO_3$ at various initial P and Fe concentrations as indicated. Data of Tiberg et al. [6]. The open symbols are duplicates in terms of initial concentrations. The lines have been calculated with the parameter set of Table 2, using a surface area A = 611 m^2 g^{-1} at a molar mass of M_{nano} = 94.8 g/mol Fe.

5 Arsenate adsorption by ferrihydrite. The adsorption of AsO_4 as a function of pH has been measured by many authors. Since Fh is rather sensitive to the way it is produced and stored before use, results may vary [7]. With modeling, a consistent set of data have been compiled that covers a wide range of conditions, such as the initial concentration (10 µM -27000 µM), the electrolyte level (0.01 M and 0.1 M), and type of background electrolyte (NaCl, $NaNO_3$, $NaClO_4$), and the Fh concentration (0.3 - 20 mM or 0.03 -2 g Fh/L). These data sets are from references [8-13].

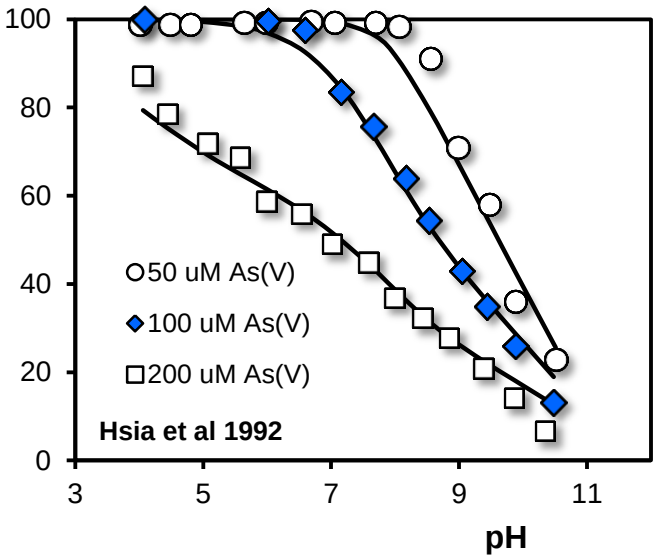

Figure S4. Effect of the initial concentration of arsenate on the relative amount of arsenate (%) bound by Ferrihydrite as a function of pH for systems with 1 mM Fe (0.095 g Fh /L) using 0.01 M $NaNO_3$ as background electrolyte. The lines have been calculated assuming A = 611 m^2 g^{-1} and M_{Fh} = 94.8 g/mol Fe.

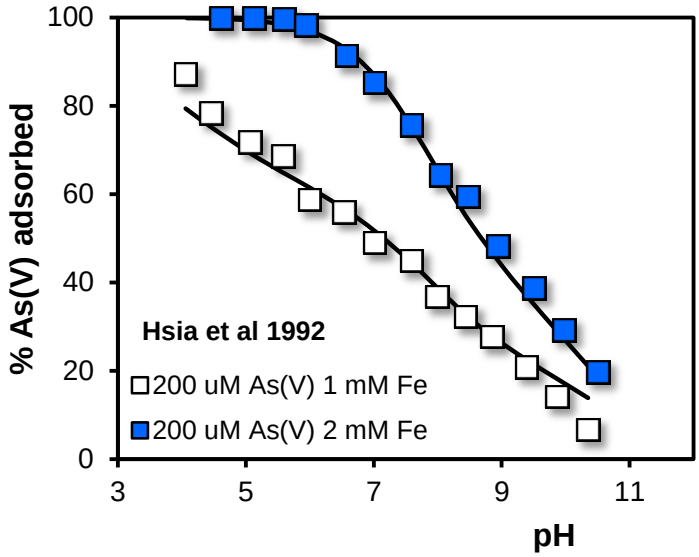

Figure S5. Effect of the Fh concentration on the relative amount of arsenate (%) adsorbed as a function of pH for systems with either 1 or 2 mM Fe (0.095 and 0.19 g Fh /L) using 0.01 M $NaNO_3$ as background electrolyte. The lines have been calculated assuming A = 611 m^2 g^{-1} and M_{nano} = 94.8 g/mol Fe.

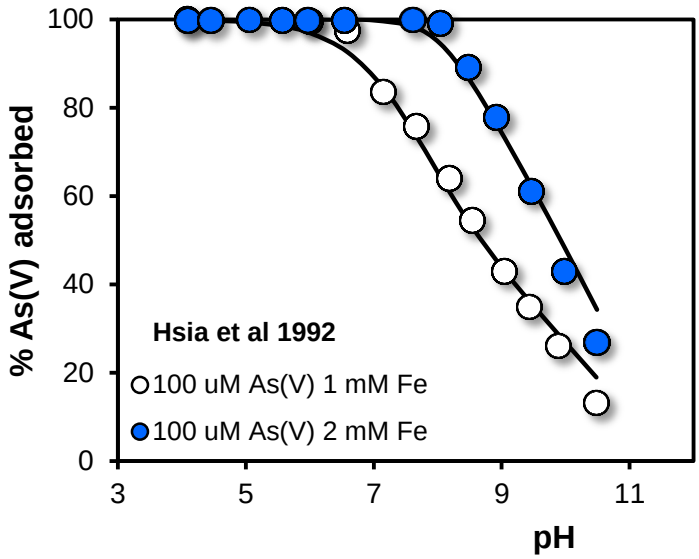

Figure S6. Same as Figure S5, but with a lower initial concentration of arsenate. The lines have been calculated assuming A = 611 m^2 g^{-1} and M_{nano} = 94.8 g/mol Fe.

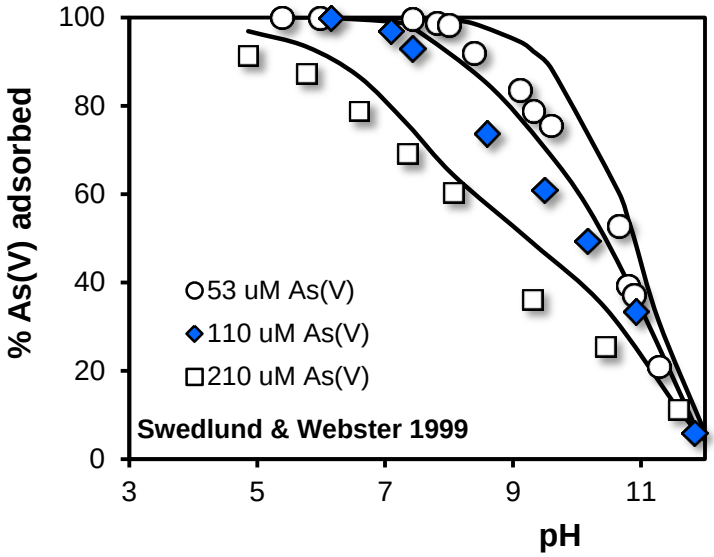

Figure S7. Adsorption edges of AsO_4 binding to ferrihydrite (1.7 mM Fe or 0.16 g Fh /L) in 0.1 M $NaNO_3$ for three initial concentrations of arsenate. The lines have been calculated assuming A = 611 m^2 g^{-1} and M_{nano} = 94.8 g/mol Fe.

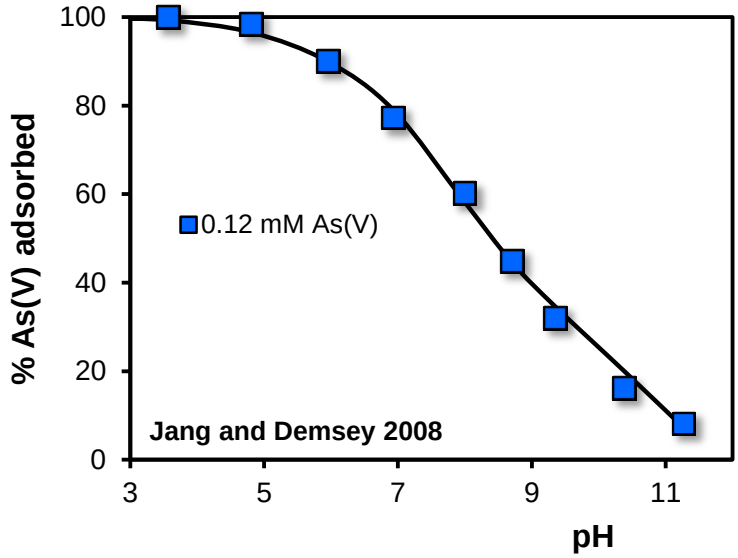

Figure S8. The relative amount adsorbed (%) as a function of pH for a system with a relatively high concentration of Fe (10 mM Fe or 0.095 g Fh /L) measured in 0.013 M NaCl. The lines have been calculated assuming A = 611 m^2 g^{-1} and M_{nano} = 94.8 g/mol Fe.

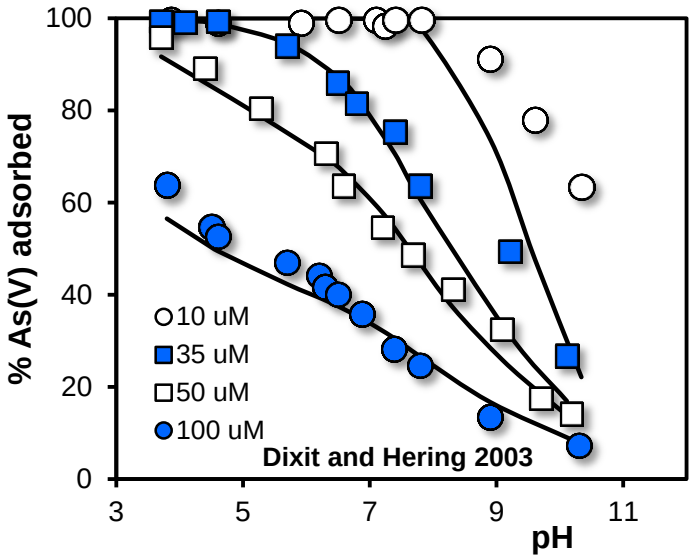

Figure S9. Effect of the initial As concentration on the relative amount of arsenate (%) adsorbed as a function of pH for a system with a relatively low concentration of Fe (0.34 mM Fe or 0.032 g Fh /L) measured in 0.01 M $NaClO_4$. The lines have been calculated assuming A = 611 m^2 g^{-1} and M_{nano} = 94.8 g/mol Fe.

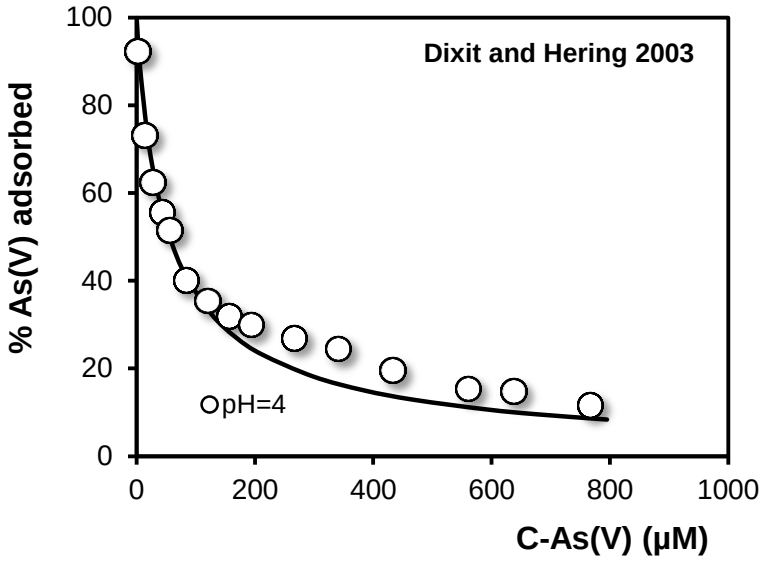

Figure S10. Relative adsorption of arsenate (%) at increase of the final concentration at pH = 4 for a system with a relatively low concentration of Fe (0.34 mM Fe or 0.032 g Fh /L) measured in 0.01 M $NaClO_4$. The lines have been calculated assuming A = 611 m^2 g^{-1} and M_{nano} = 94.8 g/mol Fe.

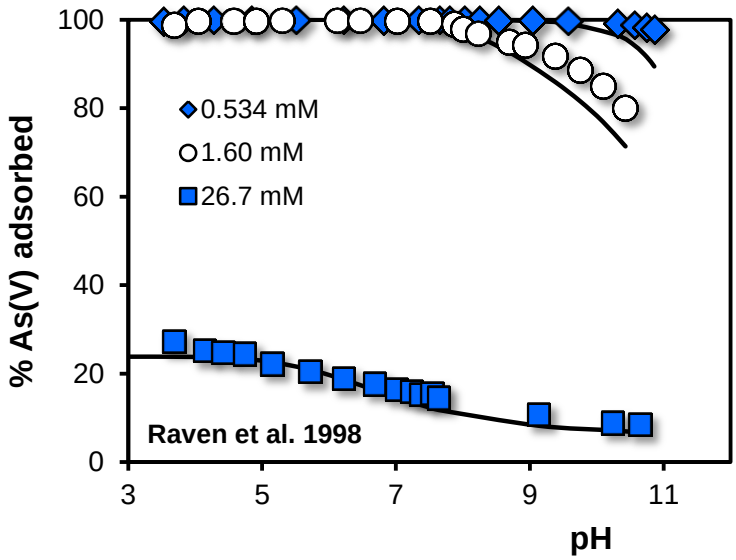

Figure S11. Effect of the initial AsO_4 concentration on the relative amount adsorbed (%) as a function of pH for a system with a relatively high concentration of Fe (20.8 mM Fe or 1.98 g Fh /L) measured in 0.1 M NaCl. The lines have been calculated assuming A = 611 m^2 g^{-1} and M_{nano} = 94.8 g/mol Fe

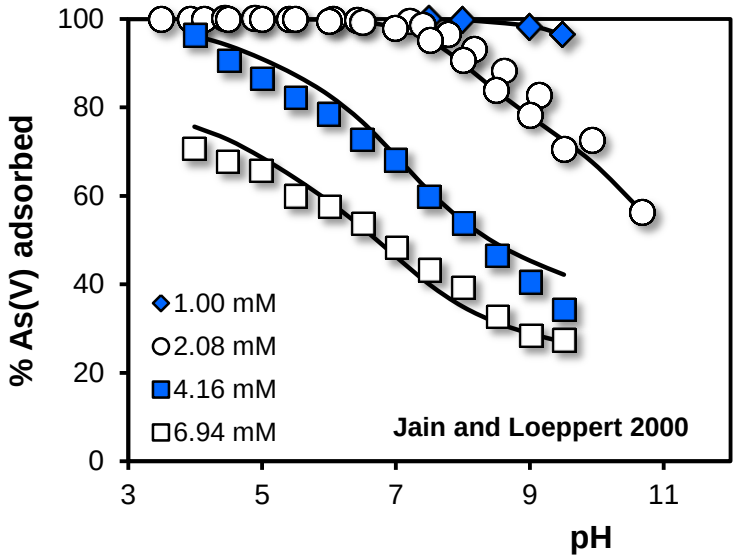

Figure S12. Effect of the initial AsO_4 concentration on the relative amount adsorbed (%) as a function of pH for a system with a relatively high concentration of Fe (20.8 mM Fe or 1.98 g Fh /L) measured in 0.1 M NaCl. The lines have been calculated assuming A = 611 m^2 g^{-1} and M_{nano} = 94.8 g/mol Fe.

6 Kinetics of PO_4 binding to *Pf*Ftn and Fh. The binding of phosphate to ferritin preloaded with 1500 Fe per mole *Pf*Ftn is given in the Figure S13 (blue spheres), showing that equilibrium can be reached within about 2 hours [14]. We have rescaled the original data of Figures 4 a,b of Sevcenco et al. [14] to be consistent the other data sets presented by these authors (published Figures 1-3). The scale (95-100%) ranges most likely from 0-100 %. The open triangles are for the adsorption to Fh formed at flash neutralization of a Fe(III) solution, showing equilibration within 1 hour.

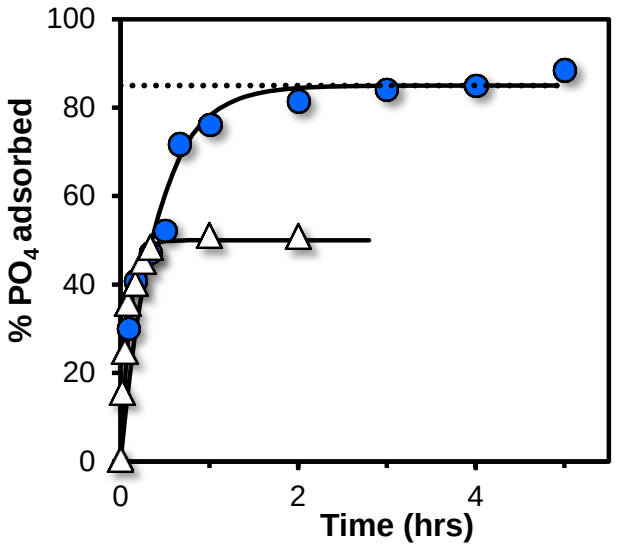

Figure S13. Relative amount of adsorbed PO_4 as a function of the time of reaction. Blue spheres are for PO_4 in a system [14] with 50 nM PO_4 and 70 nM Ftn loaded with 1500 Fe/*Pf*Ftn (mol mol^{-1}). Triangles are for a system with 500 µM PO_4 and 1 mM Fe(III) formed by fast neutralization [15]. The data are described assuming a single solid phase reacting according to a first order kinetic reaction with a rate constant of respectively k = 2.5 h^{-1} and k = 10 h^{-1}. In less than 1-2 hours, equilibrium is reached.

The adsorption rate of Ftn can be described with a single first order reaction according to $Q/Q_{max} = 1 - \exp(-k\,t)$ in which the rate constant k ~2.5 h^{-1} and Q_{max} is the maximum adsorption percentage at equilibrium (85 %).

In case of PO_4 binding by Fe hydroxide polymers prepared by very fast (1 minute) neutralization of a Fe(III) solution at pH=7, a higher rate constant is found (k ~10 h^{-1}). Equilibrium is reached within 1 hour [15]. The difference in rate constant might be due to the influence of the cage of Ftn on the reaction rate. Another possibility is that very tiny nuclei produced with flash (1 minute) neutralization are still growing during the equilibration. In that case, the phosphate adsorption equilibrium will be reached faster.

7 PO_4 adsorption isotherms of flash-fast produced Fh. In Figure S14, the phosphate adsorption isotherms has been given for instantaneously neutralized Fe(III) solutions in 0.1 M NaCl / 2 mM $NaHCO_3$ at pH=7 (MOPS) that has been aged for 1 minute, 8.5 hours, or 24 hours in advance. Data of Mao et al. [15]. For describing the phosphate adsorption data, only the specific surface area (m^2/mol Fe) has been fitted using the parameterized CD model.

The added 2 mM $NaHCO_3$ may interact with the Fh particles. The carbonate can form binuclear bidentate complexes with $FeOH(b)^{-1/2}$ groups according to the reaction:

$$2 \equiv \mathrm{FeOH(b)}^{-\frac{1}{2}} + 2\ \mathrm{H^+(aq)} + \mathrm{CO_3^{3-}(aq)} \leftrightarrow \equiv(\mathrm{FeO})_2^{-0.38}\mathrm{CO}^{-0.62} + 2\ \mathrm{H_2O(l)} \quad \log K_{\mathrm{B,CO3}} \qquad \text{(S2)}$$

The reaction has been quantified previously ($\log K_{BCO3}$ = 21.5) [16]. The charge distribution coefficients Δz_0 = +0.62 and Δz_1 = -0.62 v.u. have been derived from the optimized geometry of a hydrated cluster.

The phosphate adsorption isotherms have been collected for relative high concentrations (~10^{-5}-10^{-3} M). In combination with a high affinity, the added PO_4 ion is a very good competitor for carbonate. The carbonate ion is hardly bound to the Fh in the systems of Figure S14, and for this reason, the presence of the $NaHCO_3$ has relatively little influence. The CD model is able to describe the PO_4 adsorption very well. The fitted values for the specific surface area are given in the Table S4. In the modeling, we used the appropriate corresponding values for molar mass, mass density, and particle size and capacitance values for the Stern layers (see Table S4). The results for pH 7 have been given in the main text as graph.

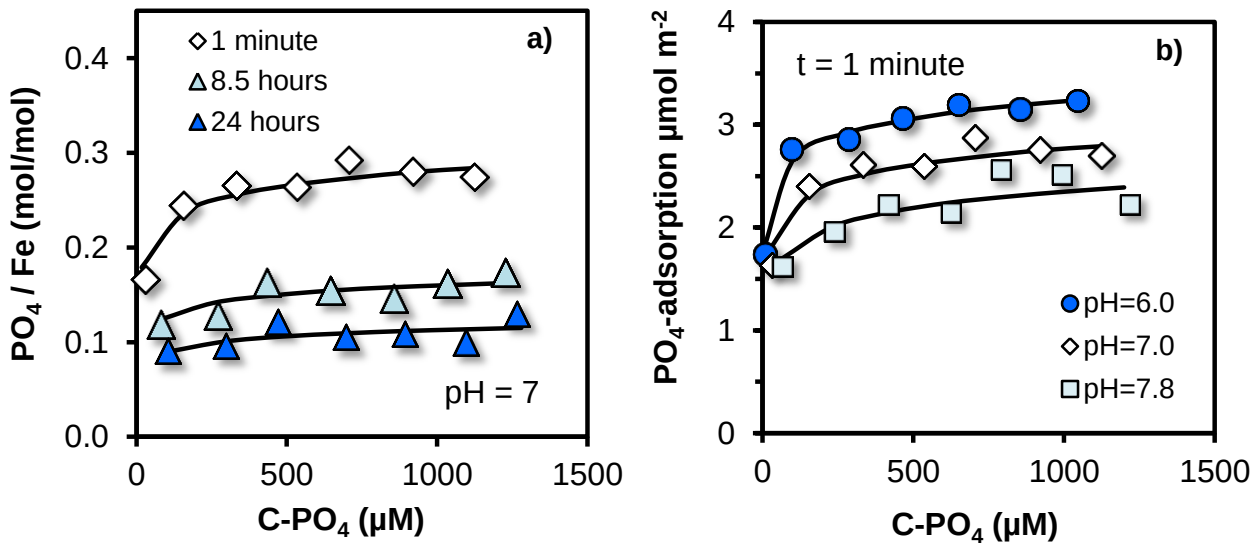

Figure S14. Adsorption isotherms of PO_4 measured for Fh instantaneously formed at pH=7 in 0.1 M NaCl by fast neutralization [15]. In Figure S14a, the effect of initial aging before PO_4 addition is shown and the adsorption is expressed in a ratio. In Figure S14b, the effect of pH is given and the adsorption is expressed per unit surface area.

Table S4. Conditions (pH, time of aging) in the experiments of Mao et al. [15] and the fitted value of the specific surface area A with error and the consistent values for the molar mass M_{nano}, mass density ρ, particle size d, average number of Fe per particle n_{Fe} and the capacitance values C_1 and C_2.

pH	Aging time	A $m^2\ g^{-1}$	M_{nano} g/mol Fe	ρ g cm^{-3}	d nm	n_{Fe}	C_1 F m^{-2}	C_2 F m^{-2}
7.0	1 minute	971 ± 6	104.7	3.40	1.82	62	1.25	0.98
7.0	8.5 hours	614 ± 8	94.9	3.80	2.57	215	1.14	0.92
7.0	24 hours	454 ± 11	91.0	4.01	3.30	500	1.09	0.89
6.0	1 minute	1028 ± 3	106.5	3.34	1.74	53	1.26	0.98
7.8	1 minute	807 ± 9	99.9	3.57	2.08	102	1.20	0.95

The phosphate adsorption isotherms have also been measured for pH 6.0 and 7.8 (Figure S14b) without no significant aging. The fitting with the CD model suggests nearly the same size of Fh particle produced at pH = 6.0 as for pH = 7.0 (Figure S15). However, for pH=7.8, the amount is apparently higher. At this condition, the particles are close to the PZC and attachments resulting in aggregation or and self-assembly may occur, particularly at a high ionic strength. Subsequently fusion may occur resulting in larger particles. Another explanation might be that the initial precipitation rate is high at a high pH.

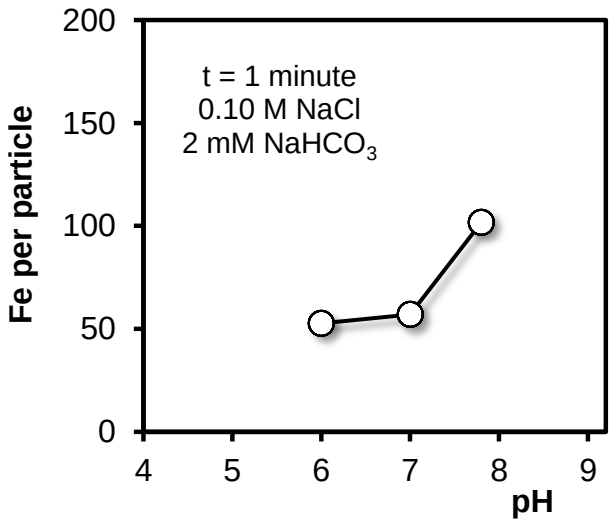

Figure S15. pH dependency of average number of Fe per Fh particle produced by instantaneous neutralization of a Fe(III) solution followed by aging for only one minute before the addition of phosphate for determining the adsorption isotherms (Figure S14b, Table S4) .

8 Specific surface area of Ferrihydrite.

Surface probing with gas molecules (BET method)

The specific surface area (SSA) of metal (hydr)oxides (m^2/g) is traditionally determined using gas adsorption (N_2, Ar, or Kr). The measured adsorption is interpreted with the BET equation and has the advantage over Transmission Electron Microscopy (TEM) observations that it directly accounts for irregularities in shape and particle porosity.

The BET method may fail when the contact area between the particles increases during the required step of dehydration for removing physically adsorbed water. Therefore, the method cannot be applied to nanoparticles such as ferrihydrite [17, 18].

Estimation of the specific surface area using H^+ as probe ion

To derive the surface area of 2LFh, Davis et al. [19] has suggested the use of protons as probe ion. The pH-dependent proton adsorption has been determined and interpreted with surface complexation modeling. The basic assumption is the value of the capacitance of the inner Stern layer, which was set to 1 F/m^2. The resulting SSA for freshly prepared Fh, aged for 4 hours was close to A = 600 m^2/g assuming a molar mass of M=89 g/mol Fe. The value has been accepted as a standard and has been widely used. The outcome of the analysis will slightly depend on the type of model used such as the 1-pK or 2-pK model, the number of sites involved, and the precise value of the constants of ion pair formation. Moreover, experimental data vary slightly between different authors. Re-evaluation with the MUSIC model [1], suggests A = 650 m^2/g at M = 89 g/mol or A = 611 $m^2/$ g at M = 94.8 g mol Fe [18]. The capacitance value was set at C_1 = 1.15 F m^{-2} to account for the size dependency of the capacitance using spherical double layer theory assuming C_1=0.9 F/m^2 for a flat iron (hydr)oxide surface [2].

Consistency with TEM

The specific surface area value (650 m^2/g at M=89 g/mol) is well in line the size (d) of freshly prepared Fh without aging measured with high-resolution TEM analysis of [17],

leading to a mean value of d ~ 2.28 nm. The mean particle has a surface area equivalent with 70 10^{+3} m^2/mol Fe or A =715 m^2/g at M = 97.5 g/mol Fe and contains n_{Fe} = 141 [18]. During an additional aging for 4 hours, this value may increase by growth of about 18 Fe per hour per particle (Fig.7), or in total by ~72 Fe, resulting in n_{Fe} = 213. This number is in excellent agreement with the mean number of Fe (n = 218) in 2LFh particles with a surface area of 650 m^2/g at M = 94.8 g/mol Fe [18] derived with H^+ is probe ion.

Phosphate as probe ion

Fh can also be probed with other ions that have a high affinity, such as the phosphate ion. Using the value of A = 650 m^2/g at M = 94.8 g/mol, the measured phosphate adsorption (mol PO_4/mol Fe) can be related to a surface loading (μmol/m^2) at a particular solution condition and described with an advanced SCM. After calibration, the phosphate adsorption measured for other Fh preparations can be derived if the change in ion adsorption with change in particle size is well captured by the model. Using this approach, the specific surface area has been derived for instantaneously neutralized Fh, having a mean size of d ~ 1.8 nm at n_{Fe} ~ 60. It will be a future challenge to verify this mean size with high resolution TEM. The particles of such an instantaneously neutralized Fh will have a size between ~1.2 and ~2.4 nm (Fig.10).

Comparison to our 2LFh preparation

Our 2LFh was prepared by Fe(III) neutralization to pH ~ 8.5. By extrapolation of the data of Mao et al [20] (Fig.S15) to pH=8.5, the initial size for our 2LFH can be estimated suggesting n_{Fe} = 140 ± 20 and this value is similar to the above value found by TEM [17]. During 4 hours of Ostwald ripening, the particles may grow by ~72 Fe to about n_{Fe} = 215 ± 20. This material will have an equivalent size of d = 2.57 ± 0.07 nm and the surface area will be A = 615 ± 20 m^2/g at M_{nano} = 94.8 ± 0.5 g / mol Fe and ρ = 3.80 ± 0.02 g cm^{-3}. These values are internally consistent with the surface area used.

9 Number of Fe per particle at homogeneous nucleation.

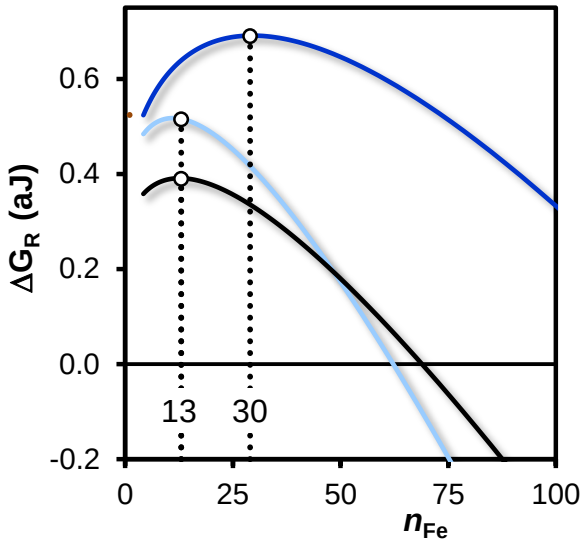

Figure S16. Gibbs free energy at formation of a Fe (hydr) oxide particle as a function of the number of iron per particle, calculated for a solution concentration that is saturated by 2LFh having a solubility product logQ_{so}= -38.3, using the surface Gibbs free energy of Fh (γ = 0.186 J m^{-2})[18] for the upper curve. For the lower black curve, the surface Gibbs free energy has been reduced by ΔG_{surf} = 0.05 J m^{-2} using the same solubility product (logQ_{so}= -38.3).
Critical nuclei are produced at the instable equilibrium condition (Ostwald-Freundlich equation) represented by curve maximum. The critical nuclei contain respectively n_{Fe} = 30 and n_{Fe} = 13.
The light blue line is the predicted curve for Fe (hydr) oxide formed at instantaneously neutralization of a Fe(III) solution, producing Fh particles containing on average 62 ± 3 Fe.
The corresponding solubility product will be logQ_{so} = -37.3 ± 0.2, which is calculated according to $\log Q_{so} = \log K_{so,\infty} + \gamma A M_{np}/2.3RT$ [18] with A (970 m^2g^{-1}) and M_{np} (104.7 g/mol Fe) as respectively the specific surface area and molar mass, and γ (0.186 J m^{-2}) as the surface Gibbs free energy. The maximum of the calculated ΔG_r curve is at n_{Fe} = 11 ± 2 for the chosen condition which fits with the size of a Fe_{13} Keggin moiety.

10 Ultra-small Fe_{20} (hydr) oxide cluster with PO_4/Fe = 0.5.

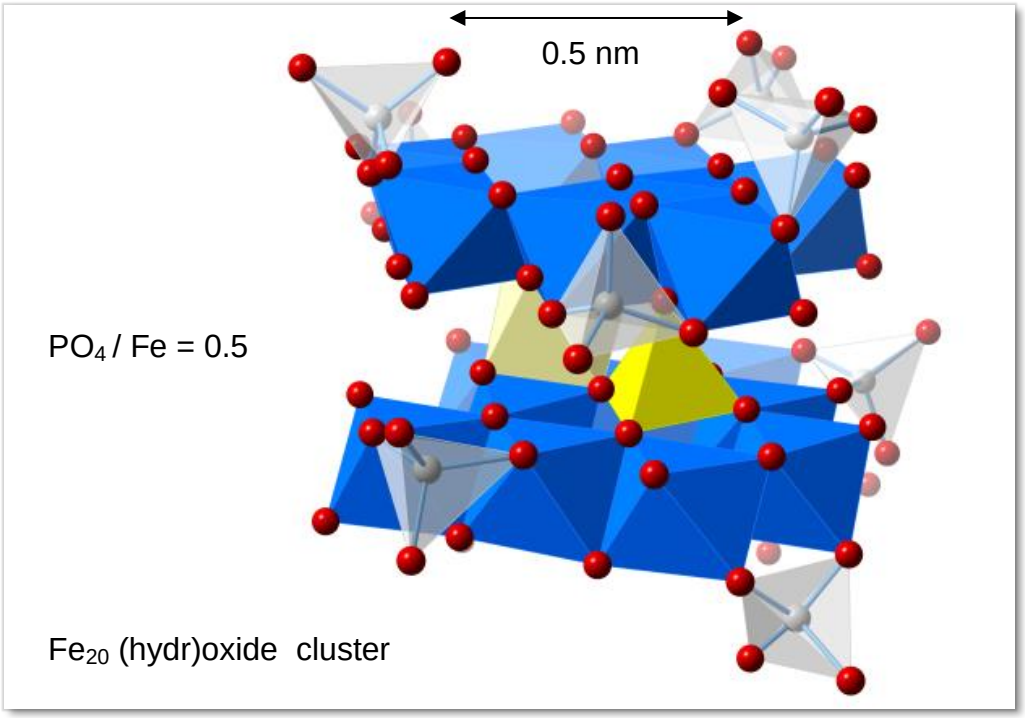

Figure S17 Graphical representation of an imaginable ultra-small Fh particle with adsorbed phosphate ions. The Fe1 octahedra are given in blue. The Fe2 and Fe3 polyhedra are in light yellow, and the phosphate tetrahedra are light colored. The oxygen ions are given as red spheres. Protons are not shown.

11 Arsenate adsorption of ferritin.

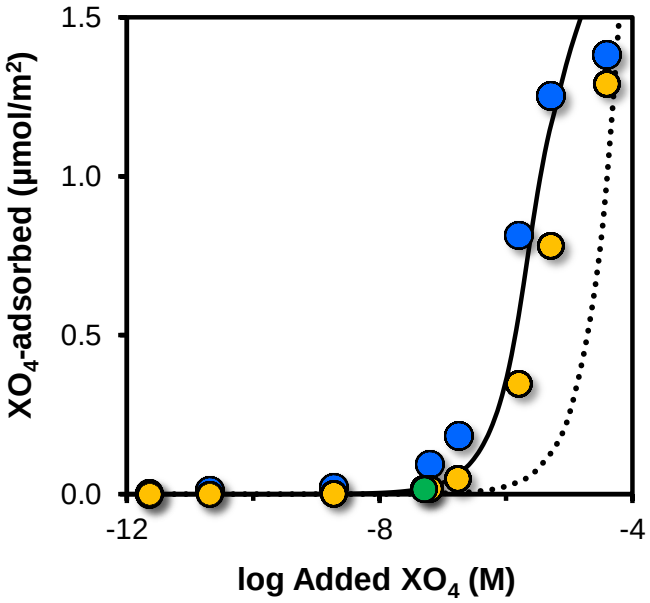

Figure S18. Calculated adsorption at pH=7 for *Pf*Ftn loaded with 1500 Fe (M = 87.8 g mol^{-1} A = 311 m^2/g), binding arsenate (dotted line) and phosphate (full line). The predictions show less affinity of arsenate for iron Ftn compared to phosphate. The spheres refer to the experimental PO_4 adsorption measured by Sevcenco et al. [14]. The blue points are based on the published data (PO_4 per Ftn (mg/g) in presented their Figure 3) and recalculated to the loading mol/m^2 using a molar mass of Ftn of 480 kD. The yellow data are based on the same experiments that were given as percentage adsorbed in their Figure 4 using a percentage scale between 95-100 %. However, it is most likely that the scale refers to 0-100%, making the data points in that case almost consistent with the numbers presented in their Figure 3 for the same experiment. The arsenate adsorption presented in their Figure 5 is completely inconsistent with the added amount of according to x-axis, suggesting much more adsorption than ever added. For this reason, these data have been omitted.

12 References.

1. T. Hiemstra and W. H. Van Riemsdijk, *Geochim. Cosmochim. Acta*, 2009a, 73, 4423-4436.
2. T. Hiemstra and W. H. Van Riemsdijk, *J. Colloid Interf. Sci.*, 2006, 301, 1-18.
3. R. P. J. J. Rietra, T. Hiemstra and W. H. Van Riemsdijk, *J. Colloid Interf. Sci.*, 2000a, 229, 199-206.
4. T. Hiemstra and W. H. Van Riemsdijk, *J. Colloid Interf. Sci.*, 1996a, 179, 488-508.
5. J. D. Kubicki, K. W. Paul, L. Kabalan, Q. Zhu, M. K. Mrozik, M. Aryanpour, A. M. Pierre-Louis and D. R. Strongin, *Langmuir*, 2012, 28, 14573-14587.
6. C. Tiberg, C. Sjostedt, I. Persson and J. P. Gustafsson, *Geochim. Cosmochim. Acta*, 2013, 120, 140-157.
7. D. A. Dzombak and F. M. M. Morel, *John Wiley & Sons: New York*, 1990, 393.
8. T. H. Hsia, S. L. Lo, C. F. Lin and D. Y. Lee, *Colloid Surf. A*, 1994, 85, 1-7.
9. K. P. Raven, A. Jain and R. H. Loeppert, *Environ. Sci. Technol.*, 1998, 32, 344-349.
10. P. J. Swedlund and J. G. Webster, *Water Res.*, 1999, 33, 3413-3422.
11. A. Jain and R. H. Loeppert, *J. Environ. Qual.*, 2000, 29, 1422-1430.
12. S. Dixit and J. G. Hering, *Environ. Sci. Technol.*, 2003, 37, 4182-4189.
13. J. H. Jang, B. A. Dempsey and W. D. Burgos, *Environ. Sci. Technol.*, 2007, 41, 4305-4310.
14. A.-M. Sevcenco, M. Paravidino, J. S. Vrouwenvelder, H. T. Wolterbeek, M. C. M. van Loosdrecht and W. R. Hagen, *Water Res.*, 2015, 76, 181-186.
15. Y. P. Mao, A. N. Pham, Y. J. Xin and T. D. Waite, *Separation and Purification Technology*, 2012, 91, 38-45.
16. T. Hiemstra, W. H. Van Riemsdijk, A. Rossberg and K. U. Ulrich, *Geochim. Cosmochim. Acta*, 2009b, 73.
17. F. M. Michel, V. Barron, J. Torrent, M. P. Morales, C. J. Serna, J. F. Boily, Q. S. Liu, A. Ambrosini, A. C. Cismasu and G. E. Brown, *Proceedings of the National Academy of Sciences of the United States of America*, 2010, 107, 2787-2792.
18. T. Hiemstra, *Geochim. Cosmochim. Acta*, 2015, 158, 179–198.
19. J. A. Davis and J. O. Leckie, *J. Colloid Interf. Sci.*, 1978b, 67, 90-107.
20. Y. P. Mao, A. N. Pham, A. L. Rose and T. D. Waite, *Geochim. Cosmochim. Acta*, 2011, 75, 4601-4610.